A Patterned TiO_2(Anatase)/TiO_2(Rutile) Bilayer-Type Photocatalyst: Effect of the Anatase/Rutile Junction on the Photocatalytic Activity

Tetsuro Kawahara, Yasuhiro Konishi, Hiroaki Tada,* Noboru Tohge, Junji Nishii, and Seishiro Ito

Semiconductor photocatalysts have recently attracted much interest because of their possible applicability to detoxification of environmental pollutants[1] and solar-energy conversion.[2] Among the photocatalysts, TiO_2 is believed to be the most promising presently known material because of its superior photoreactivity, nontoxicity, long-term stability, and low price. The photocatalytic activity of TiO_2 depends on various parameters, including crystallinity, impurities, surface area, and density of surface hydroxy groups; however, the most significant factor is its crystal form.[3] TiO_2 is usually used as a photocatalyst in two crystal structures: rutile and anatase. Anatase generally has much higher activity than rutile.[4] More interesting is the fact that the activity of P-25 (Degussa), which consists of anatase and rutile (4/1 w/w), exceeds that of pure anatase in several reaction systems.[3b, 5] Indeed, P-25 has frequently been used as a benchmark for photocatalysts.

However, the origin of the high photocatalytic activity of P-25 remains unclear. Here we report on the fundamental mechanism and present a highly active photocatalyst film designed on the basis thereof. Thin films of photocatalysts not only serve as models of particulate systems but also aid in the development of their applications.[1b]

Addition of 1-phenyl-1,3-butanedione ($BzCH_2Ac$) to a solution of $Ti(OC_4H_9)_4$ in methanol led to a red shift of the absorption peak for the $\pi-\pi^*$ transition of $BzCH_2Ac$ from 310 to 360 nm, owing to chelation of Ti^{4+}. After hydrolysis, the resultant sol was used to form a gel film in which the chelate bonds were kept intact. Significant lower solubility of the gel film in alcohol was induced by photoexcitation of the $\pi-\pi^*$ absorption band.[6] Patterned (pat-) TiO_2 films were prepared by utilizing this phenomenon. The dimensions of the patterning are expressed by the width w of the stripes of the TiO_2 film and their spacing s. Figure 1 shows a 3D surface-structure photograph of a sample formed on quartz by using a photomask with slits of 0.2 mm in width. Regularly spaced,

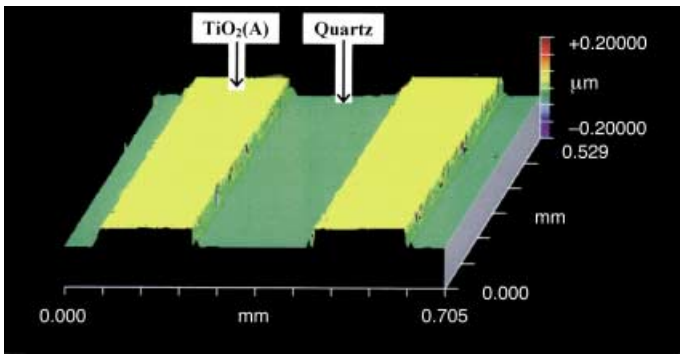

Figure 1. Three-dimensional surface-structure photograph of pat-TiO_2(A)/quartz ($w = s = 0.2$ mm).

0.2 mm wide stripes of TiO_2 film with a thickness of about 65 nm are present on the substrate with a spacing of 0.2 mm (TiO_2/quartz; $w = s = 0.2$ mm).

X-ray diffraction (XRD) patterns are shown in Figure 2 A for a sputter-deposited TiO_2 (sp-TiO_2) film (a) and a sol–gel TiO_2 (sg-TiO_2) film overlaid on the sp-TiO_2 film (b). In pattern (a), the diffraction peaks from the (110) and (211)

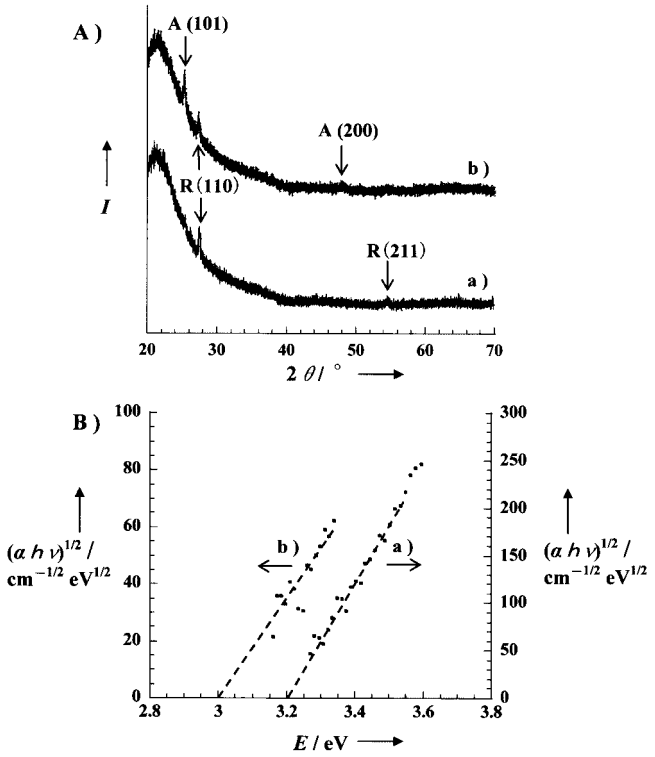

Figure 2. A) X-ray diffraction patterns of the sp-TiO_2 film (a) and the sg-TiO_2/sp-TiO_2 film (b). B) Plots of $(\alpha h\nu)^{1/2}$ vs photon energy for the sg-TiO_2 (a) and sp-TiO_2 (b) films.

planes of rutile are observed at $2\theta = 27.4$ and 54.3°, respectively. The peak intensity ratio $I(211)/I(110)$ is much smaller than that of randomly oriented rutile powder (ca. 0.6)[7] and suggests that the sp-TiO_2 film has a preferred orientation towards the [001] and [$\bar{1}$10] directions. In pattern (b), the diffraction peaks from the (101) and (200) planes of anatase appear at 25.3 and 48.0°, respectively, in addition to the rutile

[*] Prof. Dr. H. Tada
Molecular Engineering Institute
Kinki University
3-4-1, Kowakae, Higashi-Osaka, Osaka 577-8502 (Japan)
Fax: (+81) 6-6721-3384
E-mail: h-tada@apsrv.apch.kindai.ac.jp
T. Kawahara
Nippon Sheet Glass Co. Ltd.
1-7, 2-Chome, Kaigan, Minato-Ku Tokyo, 105-8552 (Japan)
Y. Konishi, Prof. Dr. N. Tohge, Prof. Dr. S. Ito
Department of Applied Chemistry
Faculty of Science and Engineering
Kinki University
3-4-1, Kowakae, Higashi-Osaka, Osaka 577-8502 (Japan)
Dr. J. Nishii
National Institute of Advanced Industrial Science and Technology
Midorigaoka1-8-31, Ikeda, Osaka 563-8577 (Japan)

  0044-8249/02/11415-2935 $ 20.00+.50/0

peaks. The broad intense background at $2\theta < 40^\circ$ in both patterns arises from the quartz substrate. Figure 2B shows the plots of $(\alpha h\nu)^{1/2}$ versus photon energy $h\nu$ for the sg-TiO_2 (a) and sp-TiO_2 (b) films; α is the extinction coefficient. Extrapolation of each straight line provides the indirect band gaps E_g of 3.2 (a) and 3.0 eV (b), which are in agreement with the literature values for anatase and rutile, respectively.[8] These results indicate that an anatase film was formed on a rutile film [TiO_2(A)/TiO_2(R)] by a two-step method consisting of sputter deposition and subsequent sol–gel processing.

Photocatalytic activities of various samples were evaluated in the gas-phase decomposition of CH_3CHO (Figure 3), which was used as a model for a harmful organic gas. This reaction is categorized as photocatalytic because both illumination

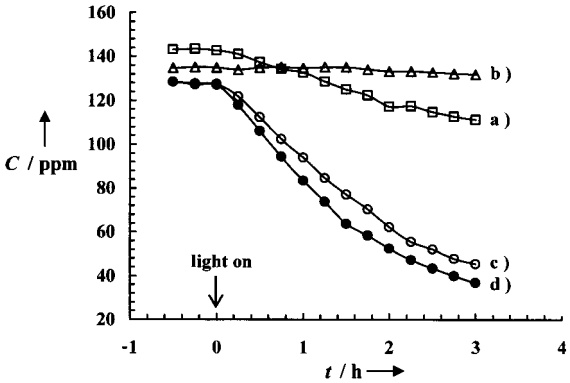

Figure 3. Time profiles of decomposition of CH_3CHO on illumination with TiO_2(A)/quartz (a), TiO_2(R)/quartz (b), pat-TiO_2(A)/TiO_2(R) ($w = s =$ 1 mm; c), and pat-TiO_2(A)/TiO_2(R) ($w = s = 0.2$ mm; d).

($\lambda_{ex} > 300$ nm) and TiO_2 are needed for decomposition to occur and the turnover number is greater than 100 at $t = 3$ h.[9] In all systems, the reaction followed a first-order rate law; Table 1 lists the apparent rate constants k. Evidently, anatase (a) exhibits higher activity than rutile (b) in this reaction. A significant increase in the activity with patterning is observed for pat-TiO_2(A)/TiO_2(R) ($w = s = 1$ mm; c), in which the rutile covers the whole surface while the anatase is deposited in stripes that leave half of the rutile underlayer exposed. The k value (0.35 h^{-1}) is larger than the sum of values of 0.091 h^{-1} for samples (a) and (b), whereas no patterning effect was obtained for TiO_2(A)/quartz.

To identify the reduction sites of pat-TiO_2(A)/TiO_2(R), the photodeposition of Ag was carried out ($2H_2O + 4Ag^+ \rightarrow 4Ag^0 + O_2 + 4H^+$).[10] Ag hardly deposited on the surface of sp-TiO_2(R). Since in the particulate system, rutile exhibits high activity in this reaction,[11] this seems to indicate sensitivity to the structure of the surface, that is, the developed (110) crystal plane of sp-TiO_2(R) is likely to be inactive. Figure 4a shows a SEM image of pat-TiO_2(A)/TiO_2(R) after Ag photodeposition. Particles are largely deposited on the

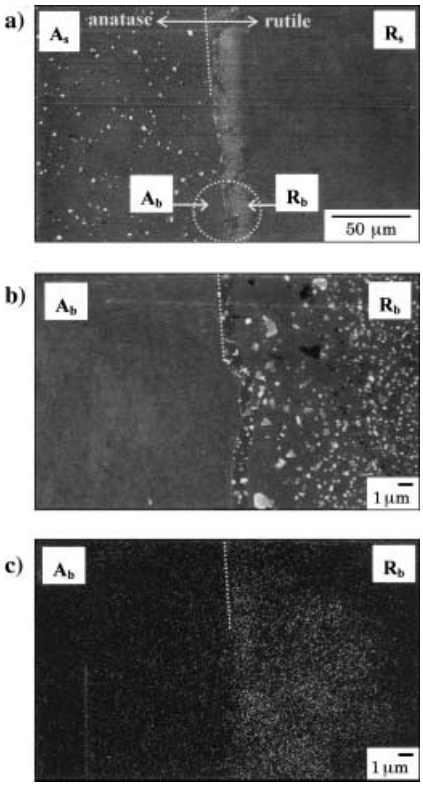

Figure 4. a) SEM image of pat-TiO_2(A)/TiO_2(R) ($w = s = 1$ mm) after Ag photodeposition. b) SEM micrograph of the boundary region of the TiO_2(A) and TiO_2(R) films; c) X-ray image of Ag for the same region as B). Ag photodeposition was performed as follows: a TiO_2-film-coated sample was immersed in a 1.0×10^{-4} M aqueous solution of $AgNO_3$ (50 mL). After the solution had been purged with Ar for 15 min, photoirradiation was carried out with a high-pressure mercury arc at $30 \pm 0.1\,^\circ C$ ($I_{320-400} =$ 2.5 mW cm^{-2}) for 0.5 h.

sg-TiO_2(A) surface (A_s), while they are scarcely seen on the sp-TiO_2(R) surface (R_s). In contrast, this trend is entirely reversed near the anatase/rutile boundary, as shown in Figure 4b, which shows a magnification of the region circled in Figure 4a, that is, deposition occurs preferentially on the side of the sp-TiO_2(R) underlayer (R_b). Figure 4c shows an Ag X-ray image of the same region as that shown in Figure 4B, which identifies the deposits as Ag. This finding shows that some of the excited electrons are transferred from the conduction band (CB) of TiO_2(A) to that of TiO_2(R), and

Table 1. Photocatalytic activities for CH_3CHO oxidation.

Photocatalyst	Surface area (R/A)	Thickness (overlayer/underlayer)	width/spacing	k [h^{-1}]
nonpat-TiO_2(R)	4 cm^2	165 ± 5 nm	–	0.005
pat-TiO_2(A)/quartz	2 cm^2	70 ± 5 nm	0.2 mm/0.2 mm	0.086
pat-TiO_2(A)/TiO_2(R)	2 cm^2/2 cm^2	70 ± 5 nm/165 ± 5 nm	1 mm/1 mm	0.35
pat-TiO_2(A)/TiO_2(R)	2 cm^2/2 cm^2	65 ± 5 nm/165 ± 5 nm	0.2 mm/0.2 mm	0.43
pat-TiO_2(A)/SnO_2[a]	2 cm^2/2 cm^2	50 ± 5 nm/580 ± 80 nm	1 mm/1 mm	0.51
pat-TiO_2(A)/SnO_2	2 cm^2/2 cm^2	45 ± 5 nm/580 ± 80 nm	0.2 mm/0.2 mm	0.53

[a] The conductivity of the SnO_2 film was 1.6×10^3 S cm^{-1}.

  0044-8249/02/11415-2936 $ 20.00+.50/0 *Angew. Chem.* **2002**, *114*, Nr. 15

the excess electrons give rise to Ag photodeposition on R_b. Another interesting fact is that the size of the Ag particles in R_b is much smaller than that in A_s, and the opposite is valid for their number density. The difference in the surface concentration of the excited electrons would affect the nucleation and growth processes of the Ag particles. The fact that the CB edge of TiO_2(A) is about 0.2 eV higher than that of TiO_2(R) is thought to facilitate interfacial electron transfer, and the energy barrier would suppress back electron transfer. Consequently, the holes left in the valence band of TiO_2(A) efficiently oxidize organic substrates, while the electrons moving into TiO_2(R) are consumed by the reduction of O_2.[12]

A closer inspection of Figure 4a indicates that Ag particles are deposited on the TiO_2(R) surface within a distance of 10 μm from the boundary. The diffusion length L of electrons in solids is related to the mobility μ and the lifetime τ by the equation $L = (kT\mu\tau/e)^{1/2}$, where k is the Boltzmann constant. Calculations with the literature values of $\mu = 100\ cm^2 V^{-1} s^{-1}$[13] and $\tau = 100$ ns[14] for TiO_2 gave an estimated L value of 5.1 μm, which is of the same order of magnitude as the width of Ag deposition. As shown in Figure 3d (see also Table 1), the activity increases by a factor of 1.23 on decreasing the patterning dimension from 1 to 0.2 mm. It is probable that the increase in the fraction of the TiO_2(R) surface acting as reduction site results in effective attack of holes on CH_3CHO adsorbed on TiO_2(A). The effect of the nanoscale junction between anatase and rutile in P-25 (ca. 10 nm)[15] on its activity can be inferred along these lines. The activity of pat-TiO_2(A)/SnO_2, which exceeds that of pat-TiO_2(A)/TiO_2(R), is almost independent of the patterning dimension (Table 1). The vectorial electron transfer from TiO_2(A) to SnO_2[16] and the long charge-separation distance of more than 100 μm[10] seem to be responsible for this.

This study has demonstrated that coupling of TiO_2(A) and TiO_2(R) in a bilayer form increases the photocatalytic activity for CH_3CHO oxidation relative to the individual components, and that reducing the patterning dimension to the charge-separation distance is of importance in increasing this activity. With regard to a model of P-25, its high photocatalytic activity is caused mainly by the increase in charge-separation efficiency resulting from interfacial electron transfer from TiO_2(A) to TiO_2(R).

Experimental Section

Patterned TiO_2 films: $BzCH_2Ac$ (40 mmol) was added to 40 mL of a 0.5 M solution of $Ti(OC_4H_9)_4$ in methanol. The solution was hydrolyzed and then used as a coating solution. Coating was carried out by dipping and withdrawing in ambient atmosphere. The dried gel films were irradiated with UV light through a photomask. An IR cut filter and a solution filter (0.40 M $CuSO_4 \cdot 5H_2O$ aq) were used to selectively pass light at around 350 nm. After the irradiated gel films had been leached out in ethanol, the resultant patterned gel films were heated in air at 773 K for 1 h.

Sputter deposition of TiO_2 films: TiO_2 thin films were deposited on quartz substrates by a conventional rf sputtering method. The sputtering target was prepared by sintering of rutile TiO_2 powder. Sputtering deposition was carried out under 1.33 Pa pressure of an O_2/Ar mixture at a growth rate of 10 nm min^{-1}. The thin film was annealed at 1073 K for 2 h in air.

Film characterization: The surface morphologies and cross sections of the TiO_2 films were observed by scanning electron microscopy (Hitachi S-700) and a 3D-imaging surface-structure analyzer (Zygo New View 100). The film thickness was also determined with the surface-structure analyzer and a surface profilometer (Dektak^3 Surface Profiler). XRD measurements were performed on a Rigaku Rotaflex RTP 300 RC.

Evaluation of photocatalytic activity: The photocatalytic activities of the samples for CH_3CHO oxidation were examined. A 508 ppm standard CH_3CHO gas was introduced into a reaction chamber (0.64 L), and diluted with air so that the initial concentration was controlled within the range 120 ± 10 ppm. After the adsorption equilibrium of CH_3CHO had been achieved in the dark, front-face irradiation ($I_{320-400} = 4.8$ mW cm^{-2}) of the sample was started with a 300 W Xe lamp at room temperature. The concentration of CH_3CHO was determined as a function of illumination time by gas chromatography (Shimadzu GC-9A; f.i.d. column Shimadzu SHINCARBON A (3 mm∅ × 3 m)). The carrier gas was N_2 (0.5 kg cm^{-2}) at an injection temperature of 70 °C and a column temperature of 70 °C.

Received: November 22, 2001
Revised: April 19, 2002 [Z18264]

[1] a) A. Mills, S. L. Hunte, *J. Photochem. Photobiol. A* **1997**, *108*, 1; b) D. A. Tryk, A. Fujishima, K. Honda, *Electrochim. Acta* **2000**, *45*, 2363.
[2] B. O'Regan, M. Graetzel, *Nature* **1991**, *353*, 737.
[3] a) H. Tada, M. Tanaka, *Langmuir* **1997**, *13*, 360; b) Z. Ding, G. Q. Lu, P. F. Greenfield, *J. Phys. Chem. B* **2000**, *104*, 4815.
[4] K. Tanaka, M. F. V. Capule, T. Hisanaga, *Chem. Phys. Lett.* **1991**, *29*, 73.
[5] a) H. Tahiri, N. Serpone, R. L. van Mao, *J. Photochem. Photobiol. A* **1996**, *93*, 199; b) J. Jia, T. Ohno, Y. Masaki, M. Matsumura, *Chem. Lett.* **1999**, 963; c) R. Zhang, L. Gao, *Mater. Res. Bull.* **2001**, *36*, 1957.
[6] N. Tohge, K. Shinmou, T. Minami, *J. Sol-Gel Sci. Technol.* **1994**, *2*, 581.
[7] JCPDS card No. 211276.
[8] H. Tang, K. Prasad, R. Sanjines, P. E. Schmid, F. Levy, *J. Appl. Phys.* **1994**, *75*, 2042. Since the position of the valence band, which mainly consists of O_{2p} orbitals, is situated at +3.0 V (vs SHE), regardless of the crystal form, the difference in E_g between anatase and rutile is almost equal to that in the conduction band edge.
[9] The turnover number was estimated by assuming that the active sites are the surface TiOH groups, whose density was reported to be about 5×10^{18} groups nm^{-2}: H. P. Boehm, *Faraday Discuss. Chem. Soc.* **1971**, *52*, 264.
[10] H. Tada, A. Hattori, Y. Tokihisa, K. Imai, N. Tohge, S. Ito, *J. Phys. Chem. B* **2000**, *104*, 4585.
[11] S.-i. Nishimoto, B. Ohtani, H. Kajiwara, T. Kagiya, *J. Chem. Soc. Faraday Trans. 1* **1983**, *79*, 2685.
[12] R. I. Bickley, *J. Catal.* **1973**, 31, 389.
[13] M. Graetzel, *Energy Resources through Photochemistry and Catalysis* (Ed.: M. Graetzel), Academic Press, New York, **1983**.
[14] R. Memming, *Semiconductor Electrochemistry*, Wiley-VCH, Weinheim, **2001**.
[15] R. I. Bickley, T. Gonzalez-Carreno, J. S. Lees, L. Palmisano, R. J. D. Tilley, *J. Solid State Chem.* **1991**, *92*, 178.
[16] Flat-band potentials V_{fb} of the SnO_2 film and TiO_2(A) film coated on soda-lime glass and Ti substrates were determined to be +0.07 and −0.34 V (vs SHE at pH 7.0 and 25 °C), respectively, from the intercepts of the Mott–Schottky plots. Direct evidence for the interfacial electron transfer is presented in ref. [10].

  0044-8249/02/11415-2937 $ 20.00+.50/0